63-3-2

TR-1108
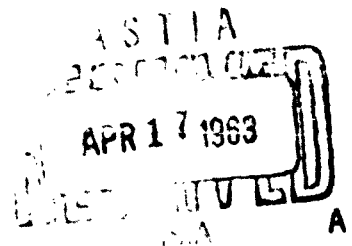
RESONANT FREQUENCIES
OF CYLINDERS OF ANY DIMENSIONS

George K. Lucey , Jr.

30 January 1963

HARRY DIAMOND LABORATORIES
FORMERLY: DIAMOND ORDNANCE FUZE LABORATORIES
ARMY MATERIEL COMMAND
WASHINGTON 25. D. C.

HARRY DIAMOND LABORATORIES

Robert W. McEvoy
LtCol, Ord Corps
Commanding

B. M. Horton
Technical Director

MISSION

The mission of the Harry Diamond Laboratories is:

(1) To perform research and engineering on systems for detecting, locating, and evaluating targets; for accomplishing safing, arming, and munition control functions; and for providing initiation signals: these systems include, but are not limited to, radio and non-radio proximity fuzes, predictor-computer fuzes, electronic timers, electrically-initiated fuzes, and related items.

(2) To perform research and engineering in fluid amplification and fluid-actuated control systems.

(3) To perform research and engineering in instrumentation and measurement in support of the above.

(4) To perform research and engineering in order to achieve maximum immunity of systems to adverse influences, including counter-measures, nuclear radiation, battlefield conditions, and high-altitude and space environments.

(5) To perform research and engineering on materials, components, and subsystems in support of above.

(6) To conduct basic research in the physical sciences in support of the above.

(7) To provide consultative services to other Government agencies when requested.

(8) To carry out special projects lying within installation competence upon approval by the Director of Research and Development, Army Materiel Command.

(9) To maintain a high degree of competence in the application of the physical sciences to the solution of military problems.

RESONANT FREQUENCIES OF CYLINDERS

OF ANY DIMENSIONS

George K. Lucey, Jr.

1

CONTENTS

ABSTRACT

Resonant frequency equations for right circular cylinders of any dimensions were derived to aid in the design of microminiature ceramic piezoelectric filters and transformers. The classical Rayleigh method was modified to include a phantom work term that accounted for energies lost to vibrations in the coupled mode. The resulting equations were

Radial mode $\qquad \left(\frac{fD}{G}\right)^2 + \left(\frac{L}{D}\right)^2 \left[\frac{4\mu_{RL} \; H \; R_o}{(1-\mu_{R\theta}) \; G \; \pi \; (1+\mu_{R\theta})^{1/2}}\right]^2 = 1$

Longitudinal mode $\left(\frac{\alpha L}{H}\right)^2 + \left(\frac{D}{L}\right)^2 \left[\mu_{RL} \frac{G \; \pi \; (1+\mu_{R\theta})^{1/2}}{2 \; H \; R_o}\right]^2 = 1$

where f and α are the fundamental frequencies; G and H are frequency constants; L and D are length and diameter; μ_{RL} and $\mu_{R\theta}$ are Poisson's ratios; and R_o is a Bessel function related to Poisson's ratio.

The equations derived were verified experimentally over a full range of dimension ratios for $BaTiO_3$ cylinders and for a small group of steel cylinders.

1. INTRODUCTION

Exact equations for determining the resonant frequencies of cylindrically shaped bodies are available in the literature for ideal one-dimensional cases, i.e. for very thin disks and small diameter rods (ref 1).

Thin disk $\qquad f_o = \frac{R_o}{\pi D} \sqrt{\frac{E_R}{\rho(1-\mu_{R\theta}^2)}}$ $\qquad\qquad\qquad$ (1)

$$R_o = (1-\mu_{R\theta})J_1(R_o)/J_0(R_o)$$

Long Rod $\qquad \alpha_o = \frac{1}{2L}\sqrt{\frac{E_L}{\rho}}$ $\qquad\qquad\qquad\qquad$ (2)

f_o = Ideal radial resonant frequency for disk with zero thickness, kc

α_o = Ideal longitudinal resonant frequency for rod with zero diameter, kc

D = Diameter, in.

L = Length, in.

E_R = Radial modulus of elasticity, lb/in.^{2}

E_L = Longitudinal modulus of elasticity, lb/in.^{3}

ρ = Density, lb-sec^2/in.^{4}

$\mu_{R\theta}$ = Poisson's ratio associating radial and tangential strains in the radial plane, dimensionless

J = Bessel function

The tiny size of microminiature piezoelectric elements usually makes the second dimension significant and the ideal handbook equations then become inapplicable. Attempts reported in the literature to take into account the effects of the second dimension are adequate only over a narrow range of length-diameter ratios.

Lord Rayleigh (ref 2) applied the principle of conservation of energy to a long, thin isotropic cylinder to derive the resonant frequency equation for the longitudinal mode. He accounted for the kinetic energy in the radial mode during longitudinal resonance by assuming that Poisson's ratio may be used to describe the radial deflections in terms of the longitudinal. He noted that the inertia of the particles was disregarded in making the assumption, but felt it would be adequate for very small diameters. Inclusion of the radial energy in the equation for conservation of energy modified the ideal longitudinal frequency equation to:

$$\alpha = \alpha_o \sqrt{1 - \frac{1}{2}\left(\frac{\mu\,\pi\,D}{2L}\right)^2} \qquad (3)$$

Mosley (ref 3) used Newton's laws and the theory of elasticity to determine the effect of length on the radial vibrations of a thick disk. However, to obtain a solution, simplifying assumptions were necessary and limited the use of his equation

$$f = f_o \sqrt{1 - \frac{1}{3}\left[\frac{R_o\,\mu\,L}{(1-\mu)\,D}\right]^2} \qquad (4)$$

to small length-diameter ratios.

In this report, the longitudinal and radial frequency equations are derived for cylinders of any dimensions. Experimental results from piezoelectric ceramic cylinders are then used to verify the equations.

2. THEORY

The modified Rayleigh procedure incorporates the following steps:

(1) Imagine that energy for _radial_ vibrations is supplied by deforming the cylinder slowly with an external pressure acting radially. Calculate the work done by this pressure.

(2) Find the energy lost to the thickness (longitudinal) mode by defining a "phantom" work as that work which would have resulted had the only existing force been a phantom force compressing the cylinder length. The phantom force as interpreted in this definition is the product of some constant N_R and the net radial force.

(3) Specify the work available for radial vibrations by subtracting the phantom work from the radial work. Assuming that the radial motion of the particles will be sinusoidal when the pressure is suddenly released, an expression for the radial resonant frequency as a function of dimensions may be derived by equating the available radial work to the maximum uncoupled kinetic energy.
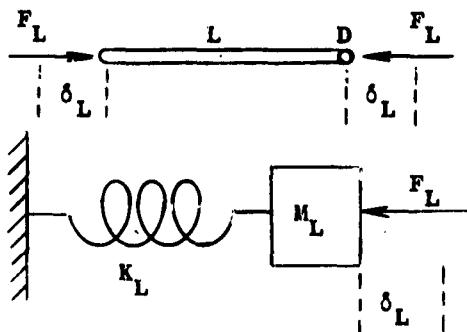
(4) An expression for longitudinal resonant frequency as a function of dimensions is derived by equating the maximum kinetic energy in the lengthwise plane and the difference between the work initially supplied to the length and a phantom work acting radially. The phantom force in this case is the product of the net longitudinal force and some constant N_L.

The conditions imposed upon the derivation to follow are:

    Right circular cylinder
    Free, undamped vibration
    Fundamental frequency
    Homogeneous material
    Planar isotropy
    Linearly elastic material
    Constant temperature

The resonant frequency equations of a right circular cylinder of any length and diameter will now be derived using a simple spring-mass analogy and the procedure outlined above. The equivalent spring constants and ideal frequencies in the derivation are presented below for the extreme cases of the cylinder, namely the thin disk and the long rod.

2.1 Spring-Mass Analogy of a Long, Thin Rod for Free Lengthwise Vibration
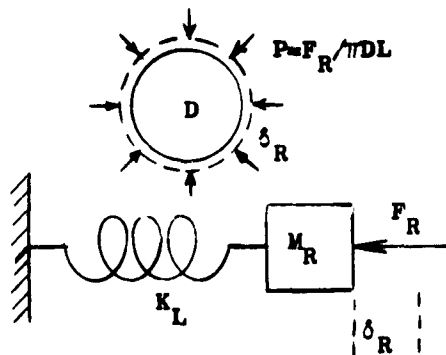

$$\delta_L = \frac{F_L(L/2)}{E_L(\pi D^2/4)} \tag{5}$$

$$K_L = \frac{F_L}{\delta_L} = \frac{E_L \pi D^2}{2L} \tag{6}$$

$$\alpha_o = \frac{1}{2\pi}\sqrt{\frac{K_L}{M_L}} = \frac{1}{2L}\sqrt{\frac{E_L}{\rho}} = \frac{H}{L} \tag{7}$$

(ref 4, p 42)

7

δ_L = Maximum longitudinal deflection, in.

F_L = Net longitudinal force, lb

K_L = Longitudinal spring constant, lb/in.

M_L = Effective lumped mass of cylinder in longitudinal vibration, lb-sec^2/in.

H = Longitudinal frequency constant, inπkc

2.2 Spring-Mass Analogy of a Thin Disk for Free Radial Vibration

$$\delta_R = \frac{F_R(1-\mu_{R\theta})}{2\pi L E_R} \qquad (8)$$

$$K_R = \frac{F_R}{\delta_R} = \frac{2\pi L E_R}{(1-\mu_{R\theta})} \qquad (9)$$

$$f_o = \frac{1}{2\pi}\sqrt{\frac{K_R}{M_R}} = \frac{R_o}{\pi D}\sqrt{\frac{E_R}{\rho(1-\mu_{R\theta}^2)}} = \frac{G}{D} \qquad (10)$$

(Ref 4, p 306)

δ_R = Maximum radial deflection, in.

K_R = Radial spring constant, lb/in.

F_R = Net radial force, lb

G = Radial frequency constant, in.-kc

M_R = Effective lumped mass of cylinder in radial vibration, lb-sec^2/in.

Effective values of E and μ are used for anisotropic materials. For piezoelectrics, the effective values are those that would be obtained experimentally with the sample fully polarized.

3. DERIVATION OF EQUATIONS

Now that the equivalent spring systems and their properties are defined, the generalized frequency equations may be derived in terms of these systems. The radial mode will be attacked first.

(1) Determine the work done on the cylinder by a tensile pressure acting in the radial direction.

$$W_{in} = \frac{1}{2} F_R \delta_R = \frac{1}{2} \frac{F_R^2}{K_R} \qquad (11)$$

8

(2) Calculate the phantom work lost to vibrations along the length. The phantom force was defined as

$$F_P = N_R F_R \qquad (12)$$

N_R = Radial constant of the phantom force

Thus the phantom work is given by

$$\frac{1}{2} W_P = \frac{1}{2} F_P \delta_L = \frac{1}{2} \frac{(N_R F_R)^2}{K_L} \qquad (13)$$

(3) Find the resonant frequency for radial vibrations.

(a) Find the work available for radial vibrations

$$\Delta W = \frac{1}{2} \frac{F_R^2}{K_R} - \frac{(N_R F_R)^2}{K_L} \qquad (14)$$

(b) Find the maximum uncoupled kinetic energy. This is found from

$$KE_{max} = \frac{1}{2} MV^2_{max} \qquad (15)$$

V_{max} = Maximum velocity of M_R

where the maximum velocity is found by differentiating the uncoupled spring displacement $\delta_r = \delta_R \cos(2\pi ft)$ with respect to time and making the result a maximum.

When this is done the maximum kinetic energy becomes

$$KE_{max} = \frac{1}{2} M_R \left(\frac{F_R}{K_R}\right)^2 (2\pi f)^2 \qquad (16)$$

(c) Equate the energies to find the frequency expression

$$\Delta W = KE_{max} \qquad (17)$$

$$f = \frac{1}{2\pi} \sqrt{\frac{K_R}{M_R}} \sqrt{1 - 2N_R^2 \frac{K_R}{K_L}} \qquad (18)$$

Introducing the spring properties (6, 9, 10) equation (18) simplifies to

9

$$\left(\frac{fD}{G}\right)^2 + \left(\frac{C_1 L}{D}\right)^2 = 1 \tag{19}$$

where

$$G^2 = \left(\frac{R_o}{\pi}\right)^2 \frac{E_R}{\rho(1-\mu_{R\theta}^2)} \tag{20}$$

$$C_1^2 = \frac{N_R^2 \; 8 E_R}{(1-\mu_{R\theta}) E_L} \tag{21}$$

(4) An analysis similar to that performed for the radial mode will show that the longitudinal frequency equation is of the form

$$\alpha = \frac{1}{2\pi}\sqrt{\frac{K_L}{M_L}} \; \sqrt{1 - \frac{1}{2}N_L^2 \frac{K_L}{K_R}} \tag{22}$$

N_L = Longitudinal constant of the phantom force.

Introducing the spring properties (6, 7, 9), the equation becomes

$$\left(\frac{\alpha L}{H}\right)^2 + \left(\frac{C_2 D}{L}\right)^2 = 1 \tag{23}$$

where

$$H^2 = \frac{E_L}{4\rho} \tag{24}$$

$$C_2^2 = \frac{N_L^2 E_L \, (1-\mu_{R\theta})}{8 E_R} \tag{25}$$

It is apparent that the radial and longitudinal equations (19,23) are incomplete mathematically in their present form in that they contain undefined constants, N_R and N_L. If left in this form the equations would be purely experimental; thus, it is necessary to break the constants into the more familiar material properties. This may be accomplished by observing the behavior of coupled modes just before free vibration occurs, and then comparing the behavior with that during free vibration.

A radial force F_R develops a deflection in the longitudinal direction due to Poisson coupling. The magnitude of the deflection of each end of the cylinder is

$$\delta_L = \frac{\epsilon_L L}{2} = \frac{\mu_{RL} F_R}{\pi D E_R} \tag{26}$$

10

ϵ_L = Longitudinal strain

μ_{RL} = Poisson's ratio relating lengthwise and radial strains.

A longitudinal force that would produce the same deflection is:

$$F_L = \frac{\epsilon_L \, \pi \, D^2 \, E_L}{2L} \qquad (6)$$

Consequently the static relationship between the lengthwise and the radial force is:

$$F_L = \left[\frac{\mu_{RL} \, D \, E_L}{2 \, \zeta \, E_R} \right] F_R \qquad (27)$$

whereas it was assumed at the beginning of the derivation that the dynamic relationship was:

$$F_P = N_R F_R \qquad (12)$$

As a result, the phantom force will be expressed as:

$$F_P = \left[\frac{\mu_{RL} \, E_L}{Y_R \, E_R} \right] F_R \qquad Y_R = \text{numerical constant} \qquad (28)$$

Thus, using equation (21)

$$N_R^2 = \left[\frac{\mu_{RL} \, E_L}{Y_R \, E_R} \right]^2 = \frac{C_1^2}{8} \, \frac{E_L}{E_R} \, (1 - \mu_{R\theta}) \qquad (29)$$

and

$$C_1^2 = \frac{4 \, \mu_{RL}^2 \, E_L}{(1 - \mu_{R\theta}) \, E_R} \qquad (30)$$

when the arbitrary assumption that $Y_R^2 = 2$ is made. Verification will be done experimentally.

Ordinarily the quantities E_R and E_L are unavailable in the literature. However, their ratio is proportional to the frequency constants G and H, which are easily obtained from literature or frequency measurements on a long rod and thin disk. C_1 should therefore be expressed in terms of the frequency constants by using equations 20 and 24.

$$C_1 = \frac{4\mu_{RL} \ H \ R_o}{(1-\mu_{R\theta}) \ G \ \pi \ (1+\mu_{R\theta})^{1/2}} \tag{32}$$

A similar analysis will show the longitudinal constant to be

$$C_2 = \frac{\mu_{RL} \ G \ \pi \ (1+\mu_{R\theta})^{1/2}}{2 \ H \ R_o} \tag{33}$$

Defining these constants completely generalizes the frequency equations 19 and 23 to functions of dimensions and material

$$\left(\frac{fD}{G}\right)^2 + \left(\frac{L}{D}\right)^2 \left[\frac{4 \ \mu_{RL} \ H \ R_o}{(1-\mu_{R\theta}) \ G \ \pi \ (1+\mu_{R\theta})^{1/2}}\right]^2 = 1 \tag{34}$$

$$\left(\frac{fL}{H}\right)^2 + \left(\frac{D}{L}\right)^2 \left[\frac{\mu_{RL} \ G \ \pi \ (1+\mu_{R\theta})^{1/2}}{2 \ H \ R_o}\right]^2 = 1 \tag{35}$$

4. VERIFICATION OF EQUATIONS

4.1 General Considerations

The equations were verified experimentally by using piezo-electric ceramic cylinders. Being piezoelectric (ref 7, p. 80), means the electrons and nuclei within the ceramic are directionally forced by the act of polarization into geometrical positions that contain no center of symmetry. Consequently, the ceramic assumes a motor or generator capability in that applying an electric field causes the body to expand or contract according to the direction of the field, and conversely, physical distortions cause the body to develop an electric charge.

Utilizing the motor ability, the body may be excited into mechanical vibration by an alternating electric field. If the field is applied at the natural resonant frequency of the body, minimum energy is required to induce maximum amplitude of vibration. The generator action of the piezoelectric being sensitive to the amplitude of strain is electrically a minimum impedance at resonance. As a

result, by noting which frequency induces a minimum impedance, the natural resonant frequency of the body is determined.

Although the piezoelectric cylinders are forced by an alternating electric field, the natural resonance is identical with that of the body in free vibration. This is true only as long as there are no external mechanical or electrical loads on the device.

The experimental procedure was to form a long piezoelectric ceramic cylinder, and then record the resonance each time part of the length was ground away. However, nothing other than the strongest fundamental was recorded because of the confusion in distinguishing the fundamental of the weak coupled mode from harmonics and subharmonics.

The experimental results were used to show that the form of the equation is correct. The material constants were then obtained experimentally from one sample and used to show that they are valid for other samples of different dimensions but of the same material. Finally, data were extracted from published literature and compared directly with the form of the theoretical equations.

4.2 Experimental Methods, Data, and Graphs

Three cylinders were made of a mixture of barium titanate and 4 percent lead titanate and were cut with an ultrasonic impact grinder in the following initial dimensions.

Sample	Diameter (in.)	Length (in.)
BT-1	0.137	0.307
BT-2	0.248	0.159
BT-3	0.147	0.359

The ends were silvered with air-drying silver paint, and then the samples were polarized longitudinally by immersing in silicone oil heated to $120^{\circ}C$, applying 40 v/mil across the samples, and allowing the oil to cool with voltage maintained. When the temperature of the oil bath dropped to about $50^{\circ}C$, the voltage was turned off, and the specimens were removed, washed, and allowed to cool to room temperature.

The samples were placed in a holder consisting of two leaf springs having a very low mechanical resonant frequency. Electrical point contact was made to the silvered surfaces of the sample under light pressure near the center of the disk. Resonant frequency determinations were made at room temperature with a Hewlett-Packard Type 606A signal generator and a Boonton Electronics Type 91B RF voltmeter as illustrated in figure 1. All resonant frequency readings were made instantly to avoid the problems of possible internal heating and frequency drift.
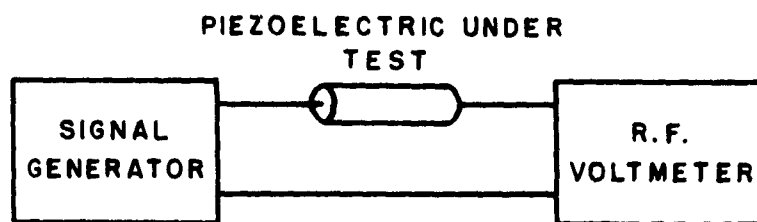
PIEZOELECTRIC UNDER
TEST

Figure 1(a) Apparatus employed for measuring the
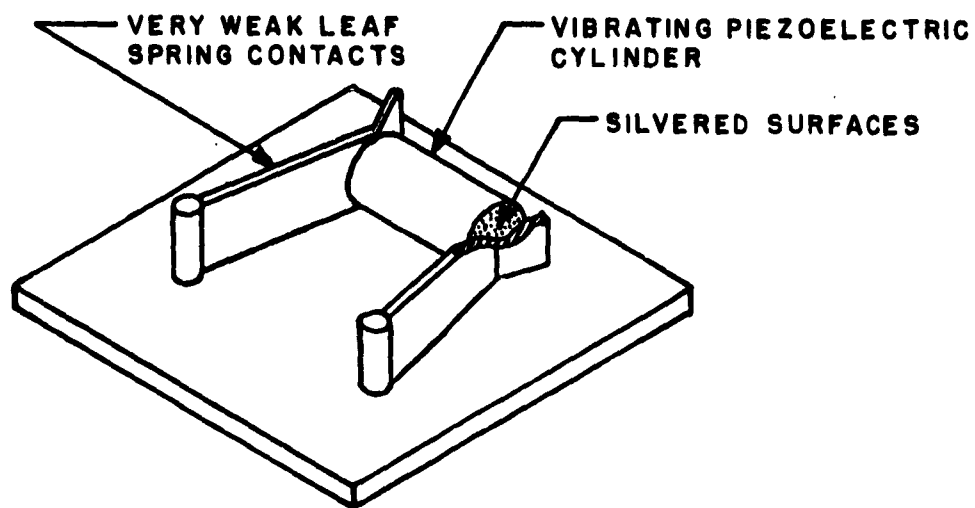resonant frequencies of piezoelectric cylinders.

Figure 1(b) Leaf spring sample holder.

The lowest frequency producing a major pip on the voltmeter was recorded for each sample. The major pip indicates an impedance change that, when related to the motor and generator action of the piezoelectric, depicts the fundamental mechanical resonance.

The samples were then ground to new lengths, the ends re-silvered, and the frequency measurements repeated. The resonances obtained are shown in table I.

Table II lists the data extracted from a publication by E. G. Shaw (ref 6) and processed into a form usable in the derived equations. Shaw's experiments were conducted on thick barium titanate disks of various diameters. His data were presented in graphical form and consequently some error in extracting the data may be expected.

Table III extracted from reference (8) p 196, is Dennison Bancroft's numerical solution to the complicated classical Pochhammer-Chree solution of the isotropic coupled longitudinal mode. A comparative table IV is obtained from the longitudinal equation derived in this report by reducing the equation to the isotropic form.

Table I. Effect of Length on Resonant Frequency

Length (in.)	Fundamental Resonant Frequency (kc)
Sample BT-1 (Diameter 0.137 in.)	
0.307	262.2
0.277	295
0.248	322.5
0.220	362.5
0.201	397
0.181	436
0.161	491
0.142	543
0.128	580
0.095	682
0.063	762
0.035	800
Sample BT-2 (Diameter 0.248 in.)	
0.159	390
0.123	419
0.079	435
0.035	455
Sample BT-3 (Diameter 0.147 in.)	
0.359	226
0.322	251.3
0.306	263.5
0.264	304.5
0.237	337

Table II. Effect of Diameter on Resonant Frequency of Thick Barium Titanate Disks Reprocessed from Reference 6.

$(L/D)^2$	$(fD)^2$ $(kc\text{-}in.)^2$	$(L/D)^2$	$(fD)^2$ $(kc\text{-}in.)^2$
1.00	5304	0.111	13440
0.640	8072	0.095	13710
0.445	10680	0.082	14040
0.326	11400	0.071	14840
0.250	11720	0.063	14330
0.197	12950	0.055	14520
0.160	12930	0.049	14310
0.132	13540	0.044	14100

Table III. Bancroft's isotropic longitudinal cross sectional frequency correction factor as a function of Poisson's ratio, μ_{RL}, and the diameter to wavelength ratio:

$$K_n = (\frac{\alpha}{\alpha_o})^2 \ ;$$

$\frac{D}{2L}$	Poisson's ratio, μ_{RL}						
	0. 1	0. 15	0. 20	0. 25	0. 30	0. 35	0. 40
0.00	1. 000	1. 000	1. 000	1. 000	1. 000	1. 000	1. 000
0.05	0. 99988	0. 99972	0. 99950	0. 99922	0. 99888	0. 99848	0. 99802
0.10	0. 99950	0. 99886	0. 99798	0. 99686	0. 99549	0. 99389	0. 99206
0.15	0. 99882	0. 99736	0. 99533	0. 99277	0. 98967	0. 98609	0. 98202
0.20	0. 99780	0. 99509	0. 99138	0. 98670	0. 98117	0. 97480	0. 96772
0.25	0. 99632	0. 99184	0. 98579	0. 97830	0. 96956	0. 95975	0. 94903
0.30	0. 99421	0. 98728	0. 97810	0. 96702	0. 95435	0. 94049	0. 92571
0.35	0. 99114	0. 98085	0. 96759	0. 95203	0. 93486	0. 91660	0. 89770
0.40	0. 98651	0. 97158	0. 95310	0. 93236	0. 91031	0. 88770	0. 86503
0.45	0. 97913	0. 95778	0. 93300	0. 90668	0. 88003	0. 85372	0. 82812
0.50	0. 96621	0. 93646	0. 90503	0. 87383	0. 84372	0. 81499	0. 78780

Table IV. Cross-sectional frequency correction factor as computed from the isotropic form of the longitudinal frequency equation derived in this report.

$$K_n = 1 - \frac{(\mu_{RL})^2}{(1-\mu_{Re})} (\frac{D}{L})^2 = (\frac{\alpha}{\alpha_o})^2$$

$\frac{D}{2L}$	Poisson's ratio, μ_{RL}						
	0. 1	0. 15	0. 20	0. 25	0. 30	0. 35	0. 40
0.00	1. 000	1. 000	1. 000	1. 000	1. 000	1. 000	1. 000
0.05	0. 99988	0. 99973	0. 99950	0. 99916	0. 99871	0. 99811	0. 99733
0.10	0. 99955	0. 99894	0. 99800	0. 99666	0. 99486	0. 99246	0. 98933
0.15	0. 99889	0. 99735	0. 99500	0. 99167	0. 98715	0. 98115	0. 97334
0.20	0. 99806	0. 99576	0. 99200	0. 98667	0. 97944	0. 96984	0. 95734
0.25	0. 99722	0. 99338	0. 98750	0. 97917	0. 96875	0. 95287	0. 93335
0.30	0. 99603	0. 99046	0. 98200	0. 97001	0. 95374	0. 93214	0. 90669
0.35	0. 99445	0. 98676	0. 97500	0. 95835	0. 93575	0. 90575	0. 86670
0.40	0. 99289	0. 98305	0. 96800	0. 94668	0. 91776	0. 87936	0. 82937
0.45	0. 99101	0. 97855	0. 95950	0. 93252	0. 89591	0. 87731	0. 78406
0.50	0. 98890	0. 97353	0. 95000	0. 91667	0. 87150	0. 81150	0. 73340

4.3 Sources of Error

Basically the sources of error are in the measurement of dimensions and frequency, and the effects of sample-holder pressure. Because of the tolerances of the ultrasonic impact grinder, a 3-mil variation in diameter occurred along the length of some cylinders. As a result, this figure was chosen to be the tolerance for length grinding. After recording the frequencies of sample BT-1 and observing the results, however, the length tolerance was reduced to 1 mil. Special attention was given to maintaining the holder pressure as light as possible on the sample, especially for long samples. Excess pressure could result in obvious changes in resonant frequency.

No extreme attention was given to the body temperature of the sample other than making a rapid frequency measurement at room temperature to avoid any drift.

Obviously, precautions such as vacuum-deposited electrodes, polished surfaces, and temperature boxes could have been instituted. It was thought, however, that an accuracy of 5 kc was all that could be expected from the instrumentation; therefore precise sample preparation was not warranted.

5. DISCUSSION

The radial and longitudinal frequencies predicted by equations 34 and 35 when plotted against length, for a constant diameter, take the form shown in figure 2. The ordinate intercept of the curve for the radial mode is the ideal frequency f_o, and the abscissa intercept is the length value at which the quantity $C_1 L/D$ becomes equal to unity. The abscissa intercept of the curve for the longitudinal mode is the length value at which the quantity $C_2 D/L$ becomes equal to unity.

The trend of the theoretical equations in figure 2 was shown to be correct by plotting the measurements made on sample BT-1 in figure 3. The right-hand portion of the curve shows that as the length of the sample was decreased, the resonance rose at an increasing rate. However, the strength of the vibration indicated on the voltmeter (fig. 1) steadily decreased to a region of lengths where two equally strong resonance readings were encountered. This was the transition region where the primary mode was switching from the longitudinal to the radial. Beyond this region, as the length was further decreased, only single strong resonances evolved, and they approached the ideal fundamental frequency as a maximum for vanishing lengths.

The compatability of the theory with the data in figure 3 may be seen readily by noting that the form of the theoretical equations is linear when the squared terms $(fD)^2$ and $(L/D)^2$ or $(\alpha L)^2$ and $(D/L)^2$ are used as coordinate axes, and that the intercepts on the axes are related to the constants of the material.

18

The figure shows axes labeled RESONANT FREQUENCY (vertical) and LENGTH (horizontal). The vertical axis marks f_0, and the horizontal axis marks $C_2 D$ and D/C_1.

LONGITUDINAL THEORY $(\alpha L/H)^2 + (C_2 D/L)^2 = 1$

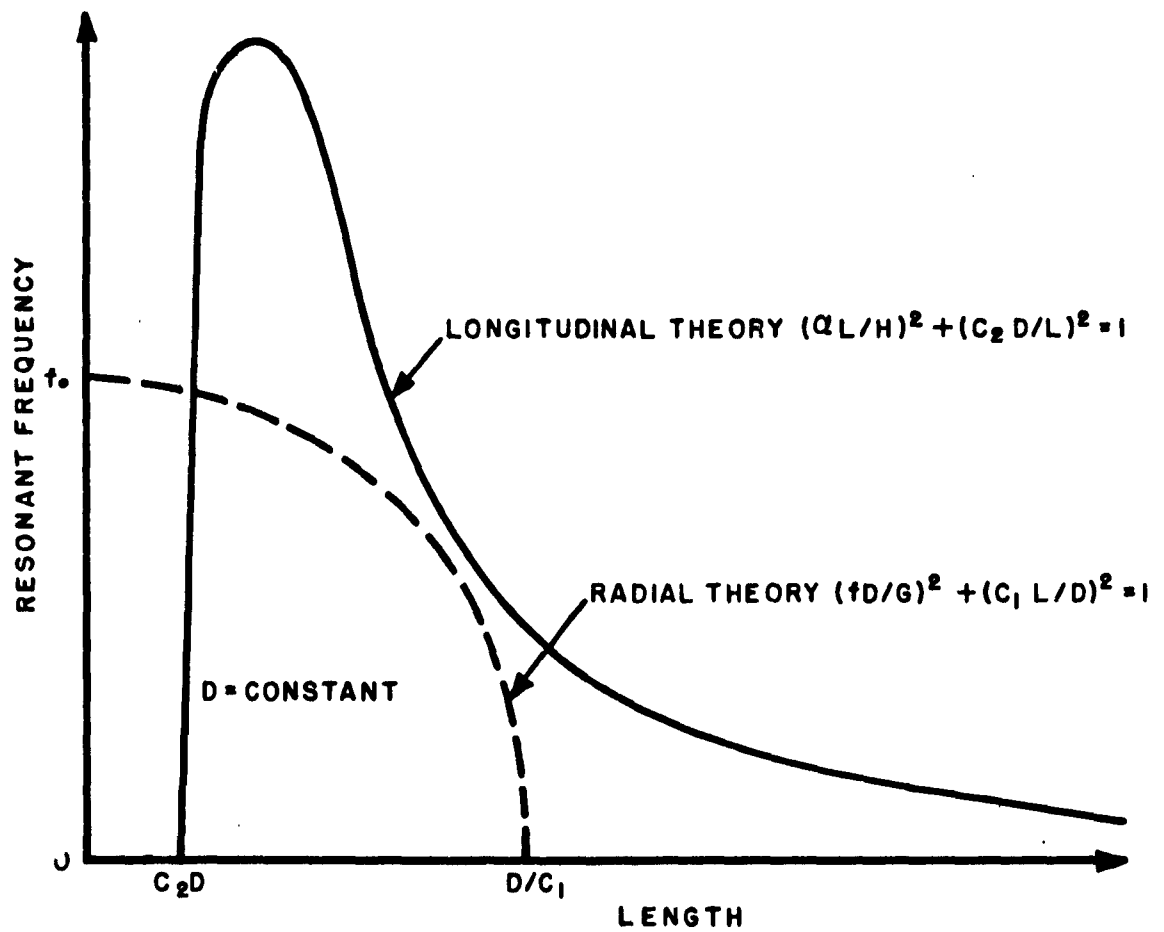RADIAL THEORY $(fD/G)^2 + (C_1 L/D)^2 = 1$

D = CONSTANT

Figure 2. Resonant frequency predicted by the modified Rayleigh equations for a cylinder of constant diameter and varying length.
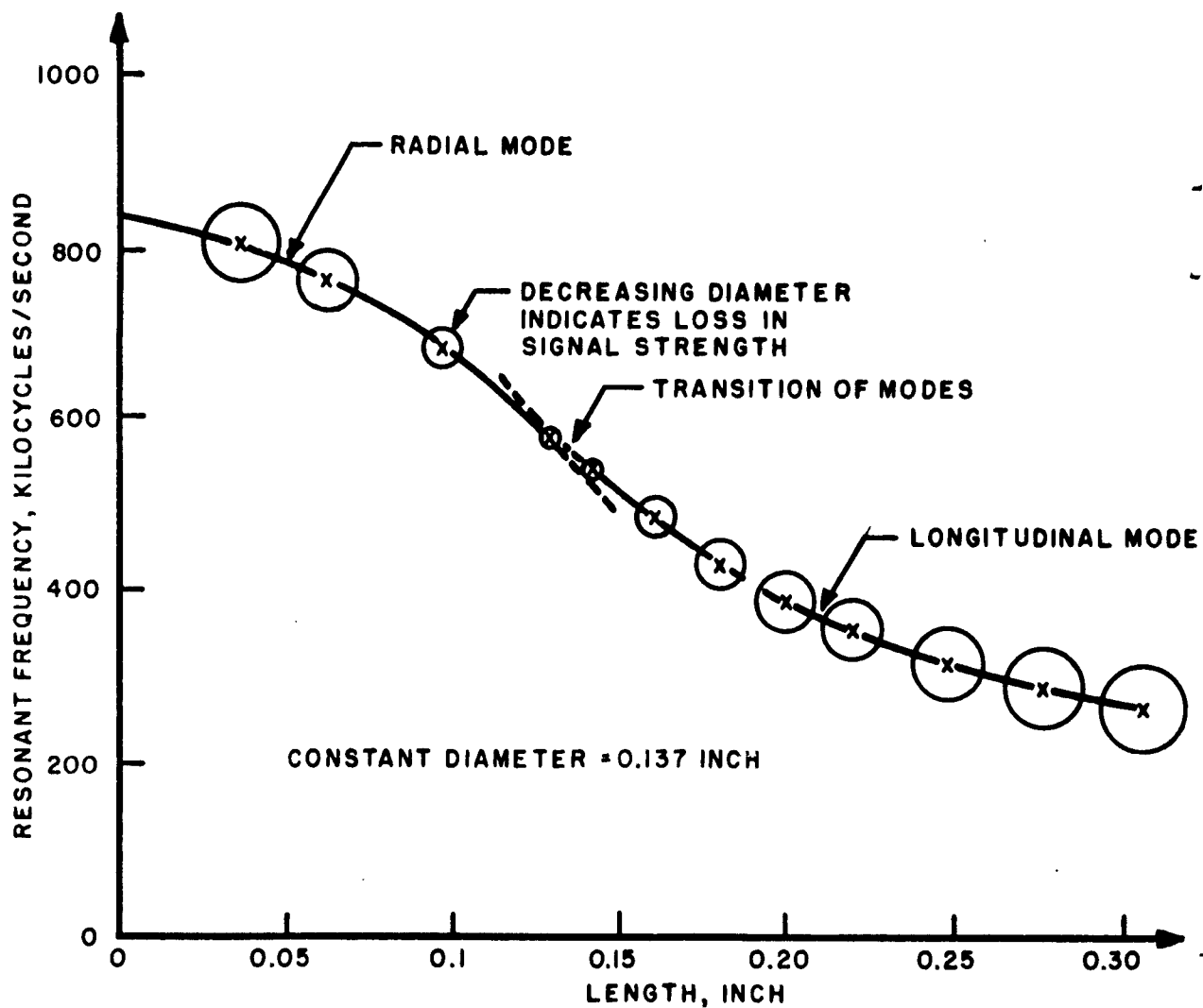
19

Figure 3. Changes in resonant frequency of sample BT-1 as the length was ground away. The curve shows a similarity to the theoretical curves given in figure 2.

Consequently if the experimental measurements are in agreement with the theory, the high frequencies of sample BT-1 plotted on the axes (resonant frequency x diameter)^2 and $(L/D)^2$ should form a straight line. The same argument applies to the low frequencies of sample BT-1; when these data are plotted on the axes (resonant frequency x length)^2 and $(D/L)^2$, a straight line should also result. Figures 4 and 5 show that this is indeed the case. Assuming then that the theory is correct, the equations may be fitted to the experimental data and the values of the constants may be calculated from the intercepts

$$G = 111.3 \text{ in.-kc} \qquad H = 82.2 \text{ in.-kc}$$

$$C_1 = 0.757 \qquad C_2 = 0.370$$

Comparative values of G and H are available in reference 1.

$$G = 111.7 \text{ in.-kc} \qquad H = 82.7 \text{ in.-kc}$$

No literature is available to provide direct comparison with the C_1 and C_2 constants. However, the components of the constants are readily available:

$$\mu = 0.3 \quad (\text{ref 7})$$

$$R_o = 2.049 \quad (\text{ref 11})$$

Inserting these values into equations 32 and 33 yields

$$C_1 = 0.726$$

$$C_2 = 0.356$$

which are in good agreement with the values 0.757 and 0.37 obtained experimentally.

As further evidence that the constants C_1 and C_2 are independent of dimensions, the measurements obtained from samples BT-2 and BT-3 were plotted in figures 6 and 7 together with the fitted equations obtained from figures 4 and 5; the degree of the fit is sufficient to warrant the conclusion that the constants are independent of dimensions.

In all experimental work reported herein, the cylinder length was the dimension varied. In an effort to verify the theory for diameter changes as well, the data presented by E. G. Shaw in reference 6 were examined for conformance to the radial theory. These data were published in graphical form so some error in extracting the data was expected; however, when they were plotted in figure 8, they followed the form of the theoretical radial equation. The intercepts differed from those obtained experimentally, and the conclusion is that a different barium titanate formulation was used by Shaw.

RESONANT FREQUENCY – DIAMETER PRODUCT SQUARED (KILOCYCLES/SECOND X INCH)²

15000

$G^2 = (111.3 \text{ KILOCYCLES/SEC} \times \text{IN})^2$

RADIAL THEORY FITTED TO THE DATA:
$[fD/111.3]^2 + [L/0.757]^2 = 1$

10000

$(1/C_1)^2 = (1/0.757)^2$

EXPERIMENTAL MEASUREMENTS

5000

CONSTANT DIAMETER = 0.137 INCH

0

0   0.1   0.2   0.3   0.4   0.5   0.6   0.7   0.8   0.9   1.0

LENGTH–DIAMETER RATIO SQUARED
$(L/D)^2$
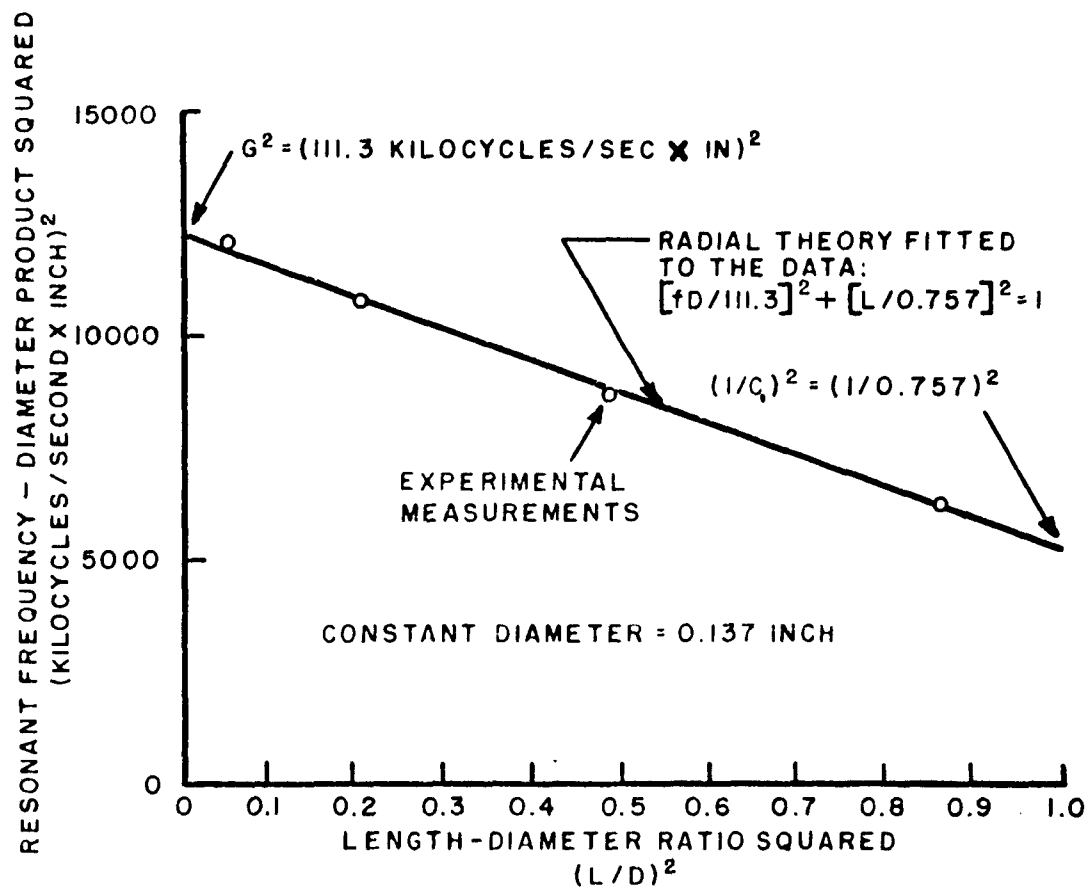
Figure 4.   High frequency data obtained from sample BT-1 illustrates the tendency of this data to follow the linear requirements of the radial equation. Fitting the radial equation to the data forces the ordinate intercept to yield the constant G^2 and the abscissa intercept the constant $(1/C_1)^2$.
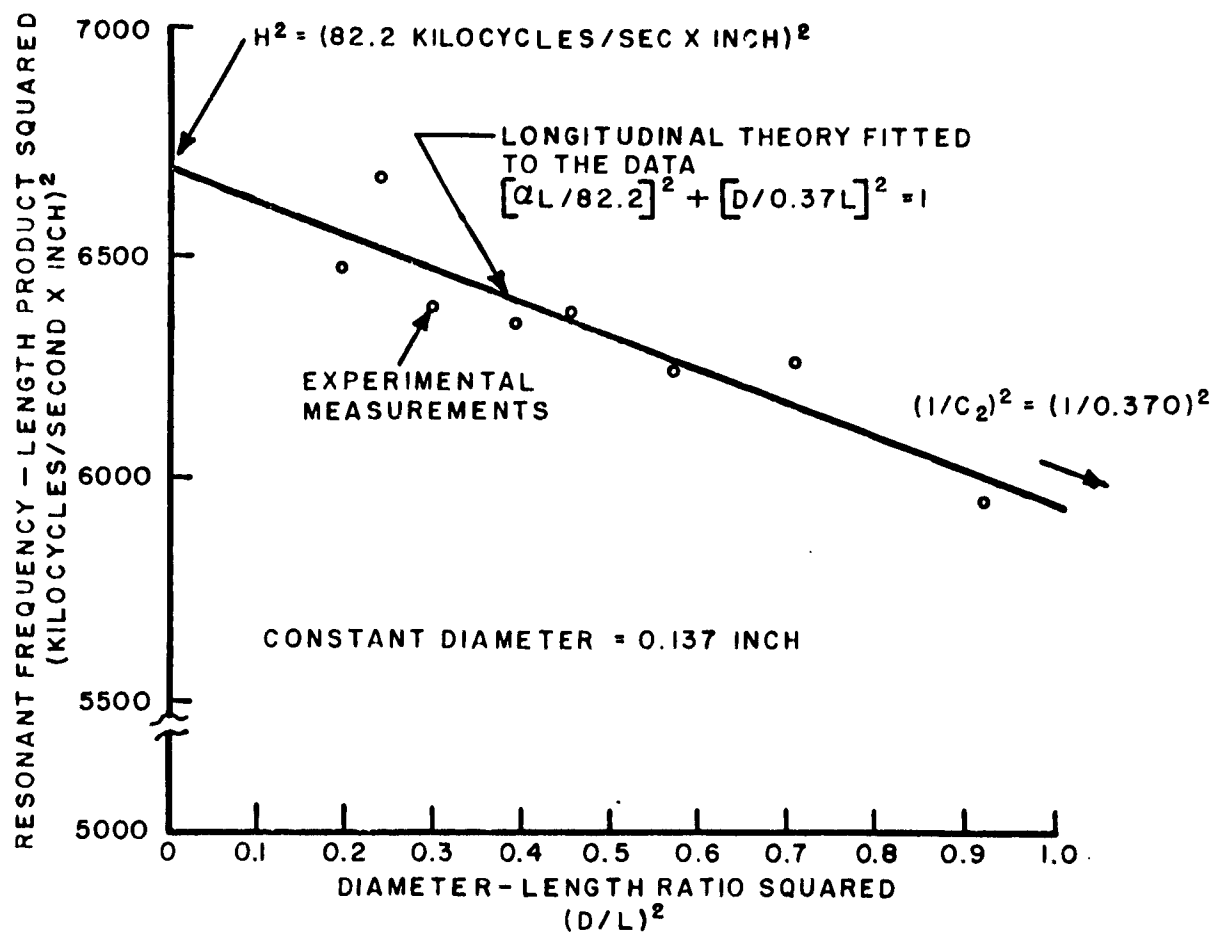
Figure 5. Low frequency data obtained from sample BT-1 illustrates the tendency of these data to meet the linear requirements of the longitudinal theory. Fitting the longitudinal equation to the data forces the ordinate intercept to represent the constant H^2 and the abscissa intercept the constant $(1/C_2)^2$.
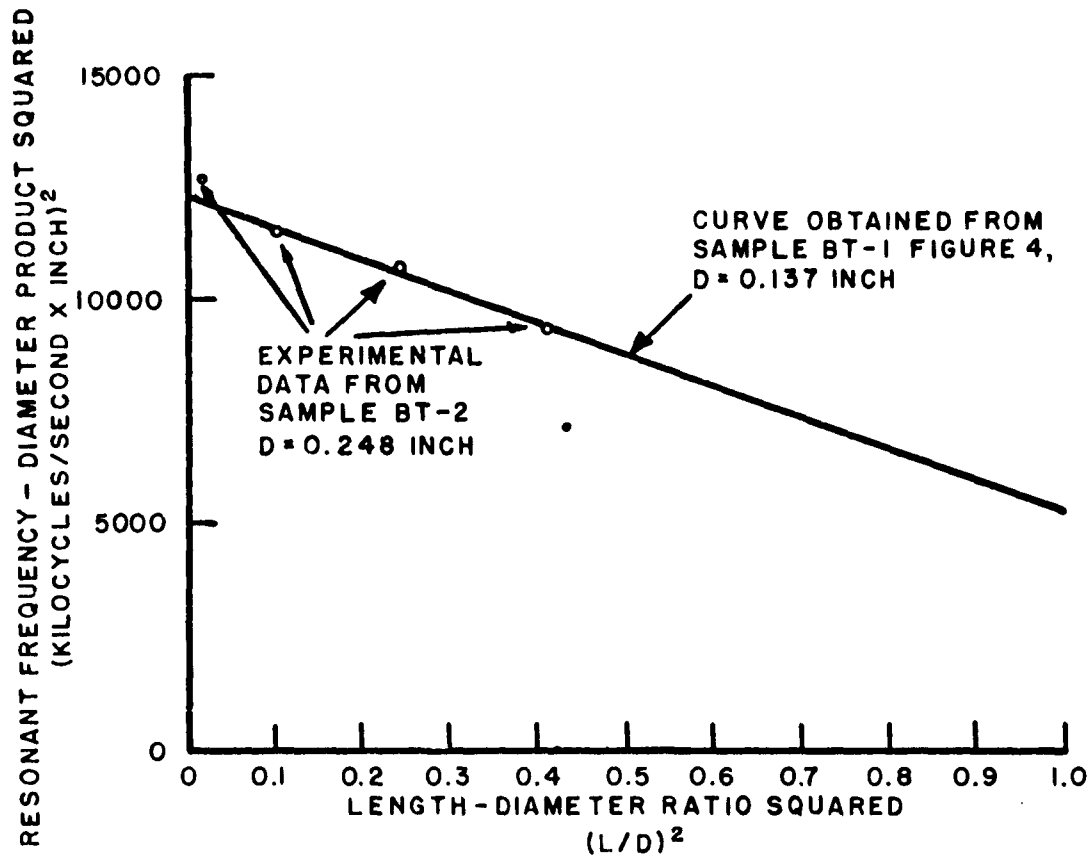
Figure 6. Plot of data for the radial mode specimens prepared from sample BT-2 (identical material to BT-1 but of a larger diameter) and the curve determined from BT-1 specimens (Figure 4). The comparison shows that the constants G and C are representative of the material and independent of cylinder dimensions.
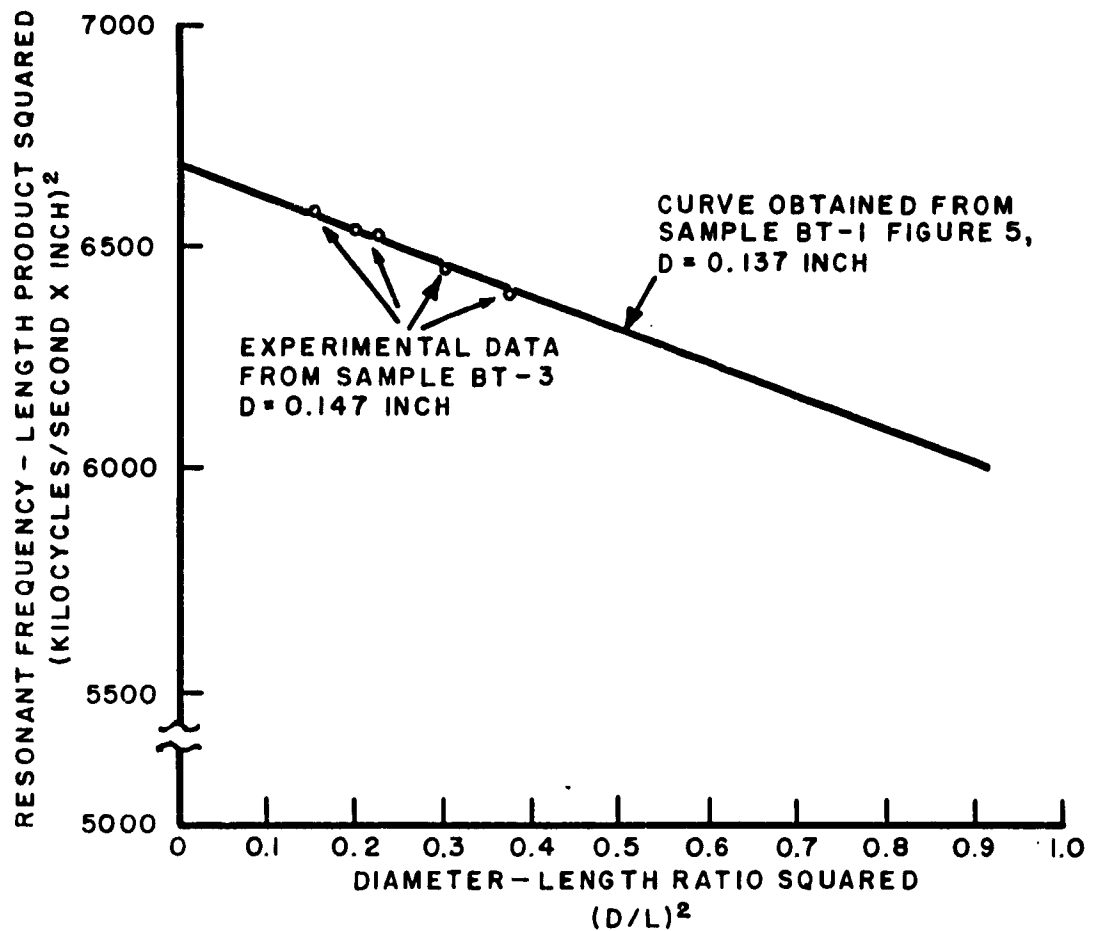
Figure 7. Plot of data for the longitudinal mode specimens prepared from sample BT-3 (identical material to BT-1, slightly larger diameter) and the curve determined from BT-1 specimens (figure 5). The comparison shows that the constants H and C_2 are representative of the material and independent of the cylinder dimensions.
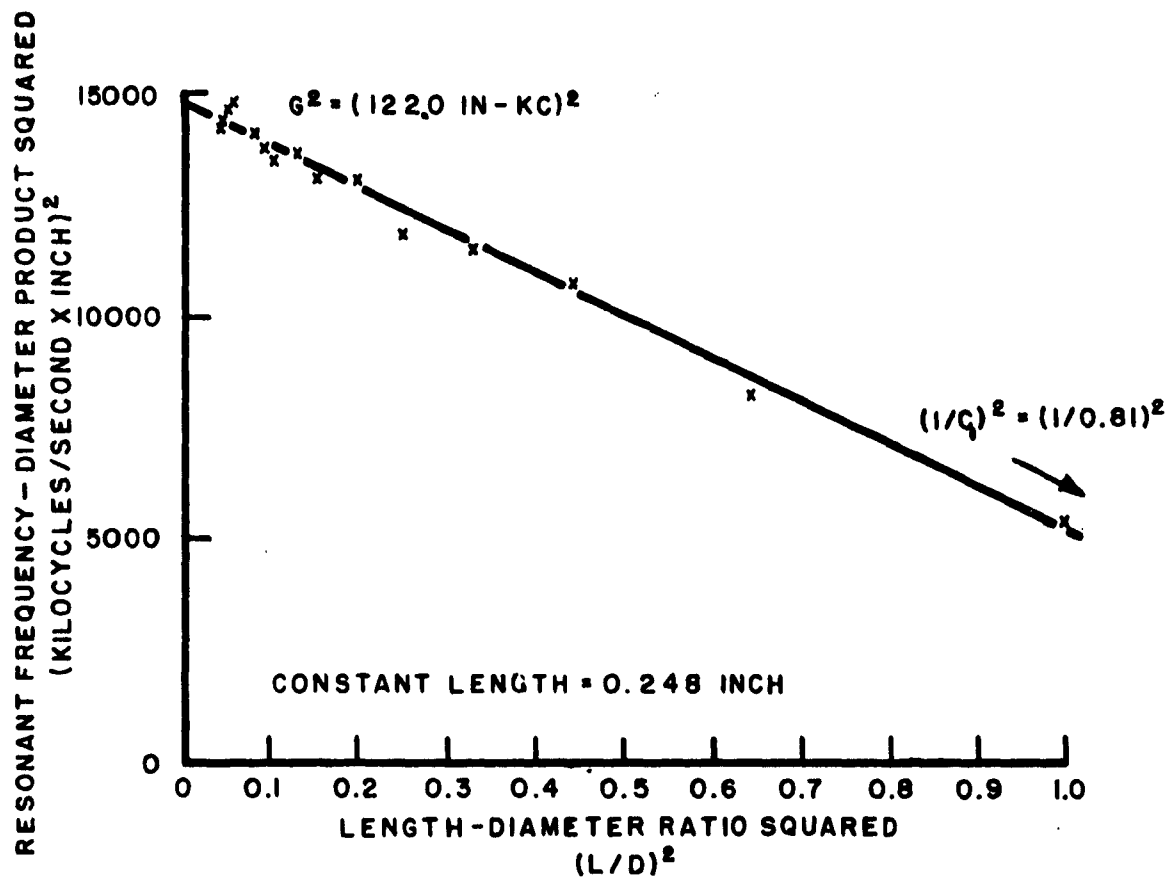
Figure 8. Reworked data from ref 6 for multidiameter cylinders also shows excellent conformity with the linear requirements of the radial equation.

Limited data were presented in reference 8, but they allowed a test of the modified Rayleigh theory on isotropic steel cylinders. Using the material properties given in the report, the constants C_2 and H were calculated, and the resulting longitudinal equation accurately predicted the resonant frequencies obtained experimentallv.

However, in all fairness it should be mentioned that more extensive data on the longitudinal vibration of steel rods was published in reference 9, page 148, which did not agree completely with the theory. In that work the claimed values of material properties did not produce correct values of H and C_2, although the linear requirements were met. The possibility that the steel was slightly anisotropic was recognized in the report, and is accepted here as the reason for deviation from the isotropic theory. Additional information was unavailable but necessary in order to employ the anisotropic equation.

Dennison Bancroft's numerical solution of the classical isotropic Pochhammer-Chree equation of the coupled longitudinal mode is listed in table III. According to this data the linear requirements of the isotropic longitudinal equation are contradicted. Table IV shows that only a slight error exists in frequency prediction between the two methods, but this error will naturally be increased as the dimension ratio approaches unity.

Figure 9 is a brief comparison of the two tables and the discrepancy cannot be explained. It will only be noted that in the region of $\mu = 0.35$ the two tables are in closest agreement, that this is the region of both the steel and piezoelectric ceramic data, that the equations developed in this paper have the advantage of being able to handle some anisotropic materials vibrating in either mode, and that all the experimental data presented in this report do appear to follow the linear requirements of the theory.

6. CONCLUSION

The experiments performed to verify the equations

$$\left(\frac{fD}{G}\right)^2 + \left(\frac{L}{D}\right)^2 \left[\frac{4 \ \mu_{RL} \ H \ R_o}{(1-\mu_{R\theta}) \ G \ \pi \ (1+\mu_{R\theta})^{1/2}}\right]^2 = 1 \tag{34}$$

$$\left(\frac{fL}{H}\right)^2 + \left(\frac{D}{L}\right)^2 \left[\frac{\mu_{RL} \ G \ \pi \ (1+\mu_{R\theta})^{1/2}}{2 \ H \ R_o}\right]^2 = 1 \tag{35}$$

showed that the trend of the equations is correct, the constants are in agreement with those in the literature for barium titanate and steel, the equations are unrestricted by anisotropic effects of piezoelectrics, and the equations are valid for any dimensions.

K_n

LONGITUDINAL CORRECTION FACTOR

1.0

ISOTROPIC LONGITUDINAL THEORY

$$\left(\frac{a}{a_0}\right)^2 = 1 - \left(\frac{\mu^2}{(1-\mu)}\right)\left(\frac{D}{L}\right)^2$$

BANCROFT

$$K_n = \left(\frac{a}{a_0}\right)^2$$

$\mu = 0.1$

$\mu = 0.35$

$\mu = 0.4$

0

0.5

$\left(\frac{D}{2L}\right)^2$

DIAMETER - WAVELENGTH RATIO SQUARED
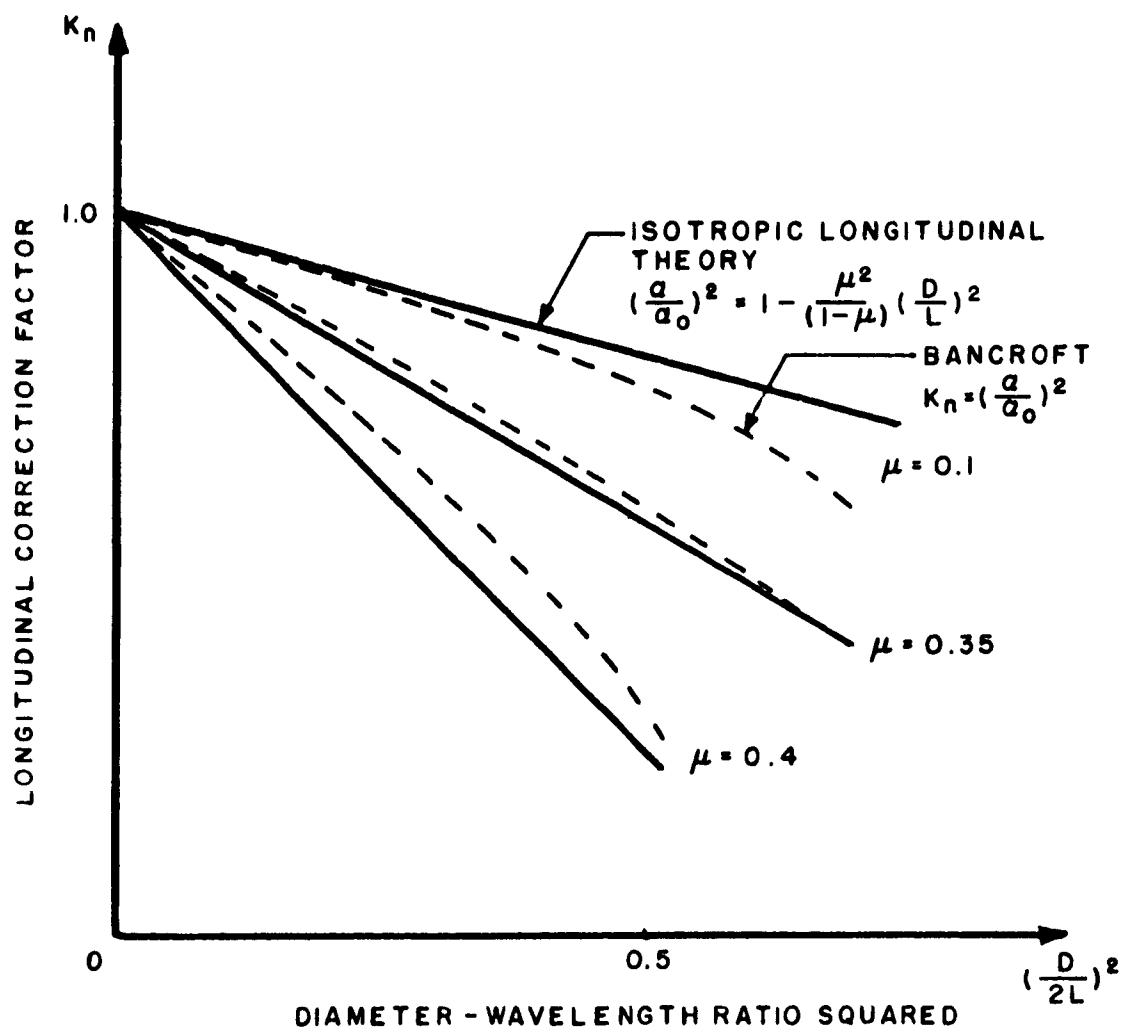
Figure 9. Comparison of Bancroft's numerical solution of coupled longitudinal vibrations with the isotropic form of the longitudinal equation derived in this report.

These equations fill a void that has hindered the design of cylindrical microminiature ceramic transformers and filters. The derivations themselves avoided the use of higher mathematics and tedious tensor equations. Their simplicity opens the door to the derivation of additional design equations that eliminate the need for the time-consuming process of experimentally determining an empirical relation.

In the field of piezoelectrics, the most valuable form of the frequency equations is:

$$\left(\frac{fD}{G}\right)^2 + C_1\left(\frac{L}{D}\right)^3 = 1$$

$$\left(\frac{\alpha L}{H}\right)^2 + C_2\left(\frac{D}{L}\right)^3 = 1$$

The constants C_1, C_2, G, and H should subsequently be listed in the literature for various materials, strengths of polarization, and temperature.

ACKNOWLEDGMENTS

Norman Doctor, Harry Diamond Laboratories, Washington, D. C. for advice and guidance.

Charles Barnett, HDL, for assistance in the verification of the theory.

John Scales, HDL, for a technical review of the report.

Dr. D. Mosley, Vitro Laboratories, Rockville, Md., for a technical review and discussion of the report.

7. REFERENCES

(1) L. A. Peterman, "Producing Motion with Magnetostrictive and Piezoelectric Transducers," Electrical Manufacturing 56, p 99, December 1955.

(2) Lord Rayleigh, "The Theory of Sound," MacMillan and Co., Ltd., New York, I, p 252, 1945.

(3) D. S. Mosley, "Contributions to the Theory of Radial Vibrations in Thin Disks," Journal of the Acoustical Society of America 32, no. 8, pp 991-995, August 1960.

(4) F. B. Seely and J. O. Smith, "Advanced Mechanics of Materials," John Wiley and Sons, Inc., New York, 1959.

(5) W. P. Mason, "Piezoelectric Crystals and Their Application to Ultrasonics," D. Van Nostrand Co., Inc., New York, 1950

(6) E. A. G. Shaw, "On the Resonant Vibrations of Thick Bariam Titanate Disks," Journal of the Acoustical Society of America ₃8, No. 1, pp 38-50, January 1956.

(7) H. W. Katz, "Solid State Magnetic Dielectric Devices," John Wiley and Sons, Inc., New York, 1959, p 534, 80.

(8) W. E. Tefft and S. Spinner, "Cross Sectional Correction for Computing Young's Modulus from Longitudinal Resonance Vibrations of Square and Cylindrical Rods," Journal of Research 66A, No. 2, March-April 1962, pp 193-197.

(9) S. Spinner, T. W. Reichard, and W. E. Tefft, "A Comparison of Experimental and Theoretical Relations Between Young's Modulus and the Flexural and Longitudinal Resonant Frequencies of Uniform Bars," Journal of Research 64A, No. 2, March-April 1960, pp 147-155.

(10) Dennison Bancroft, "The Velocity of Longitudinal Waves in Cylindrical Bars," Physical Review, Vol 59, pp 588-593 (1941).

(11) Staff of the Computation Laboratory, "Tables of the Bessel Functions of the First Kind of Orders Zero and One," Howard University Press, Cambridge, Mass, 1947.

SYMBOL GLOSSARY

		Equation No.
C_1	Grouping of radial material constants, dimensionless	32, 19
C_2	Grouping of longitudinal material constants, dimensionless	33, 23
D	Diameter, in.	1
E_L	Longitudinal modulus of elasticity, $lb/in.^2$	2
E_R	Radial modulus of elasticity, $lb/in.^2$	1
f	Actual radial resonant frequency, kc	34
f_o	Ideal radial resonant frequency for disk with zero thickness, kc	1
F_L	Net longitudinal force, lb	6
F_P	Net phantom force, lb	12
F_R	Net radial force, lb	9
G	Radial frequency constant, in.-kc	10
H	Longitudinal frequency constant, kc	7
K_L	Longitudinal spring constant, lb/in.	6
K_R	Radial spring constant, lb/in.	9
KE_{max}	Maximum kinetic energy, in.-lb	15
L	Length, in.	2
M_L	Effective lumped mass of cylinder in longitudinal vibration, $lb/sec^2/in.$	7
M_R	Effective lumped mass of cylinder in radial vibration, $lb/sec^2/in.$	10
N_L	Longitudinal constant of the phantom force, dimensionless	22
N_R	Radial constant of the phantom force, dimensionless	12, 30
W_{in}	Input work, in.-lb	11
W_p	Phantom work, in.-lb	13
ΔW	Work available for radial vibrations, in.-lb	14
α	Actual longitudinal resonant frequency, kc	35
α_o	Ideal longitudinal resonant frequency for rod with zero diameter, kc	2
δ_L	Maximum longitudinal deflection, in.	5
δ_r	Intermediate radial deflection, in.	15
δ_R	Maximum radial deflection, in.	8
ρ	Density, $lb\text{-}sec^2/in.^4$	7, 10

SYMBOL GLOSSARY (Cont'd)

DISTRIBUTION

Commanding General
U. S. Army Materiel Command
ATTN: AMCCG
Washington 25, D. C.

Commanding General
U. S. Army Materiel Command
ATTN: AMCDC
Washington 25, D. C.

Commanding General
U. S. Army Materiel Command
ATTN: AMCSA-SC
Washington 25, D. C.

Commanding General
U. S. Army Materiel Command
ATTN: AMCRD-TI
Washington 25, D. C.

Commanding General
U. S. Army Materiel Command
ATTN: AMCRD-PP
Washington 25, D. C.

Commanding General
U. S. Army Materiel Command
ATTN: AMCRD-RS
Washington 25, D. C.

Commanding General
U. S. Army Materiel Command
ATTN: AMCRD-DE
Washington 25, D. C.

Office of the Director of Defense Research and Engineering
The Pentagon, Washington 25, D. C.
ATTN: Technical Library (rm 3E1065) - 2 copies

Commanding General
Frankford Arsenal
Philadelphia 37, Pennsylvania

Commanding General
Aberdeen Proving Ground, Maryland
ATTN: ORDBG-LM, Tech. Library (Bldg. 313) - 2 copies
ATTN: Tech Library, Br No. 3, Bldg. 400, D and P Services

Commanding Officer
Picatinny Arsenal
Dover, New Jersey
ATTN: Feltman Research and Engineering Labs

Commanding General
Ordnance Weapons Command
Rock Island, Illinois
ATTN: ORDOW-IE

Commanding Officer
U. S. Army Signal Research and Development Laboratory
Fort Monmouth, New Jersey
ATTN: Electronic Components Research Dept

Commanding Officer
U. S. Army Research Office
Duke Station
Durham, North Carolina

Office for the Asst Chief of Staff for Intelligence
The Pentagon, Washington 25, D. C
ATTN: Mail and Records Branch

Ordnance Technical Intelligence Agency
Arlington Hall Station
Arlington 12, Virginia

Commanding General
Engineer Research and Development Laboratories
U. S. Army
Fort Belvoir, Virginia
ATTN: Technical Documents Center

Commanding General
Headquarters, USCONARC
Fort Monroe, Virginia

Commanding General
Ordnance Tank-Auto Command
1501 Beard Street
Detroit, Michigan

Commanding Officer
Camp Detrick
Frederick, Maryland

Department of the Navy
Chief of Naval Operations
The Pentagon, Washington 25, D. C.
ATTN: Research and Development

Department of the Navy
Washington 25, D. C.
ATTN: Chief, Office of Naval Research (Bldg T-3)

Commander
U. S. Naval Ordnance Laboratory
White Oak, Silver Spring 19, Maryland

Department of the Navy
Bureau of Naval Weapons
Washington 25, D. C.
ATTN: DLI-3, Technical Library

Commander
Naval Research Laboratory
Washington 25, D. C.
ATTN: Solid-State Electronics Br., S. Paull

Commander
U. S. Naval Ordnance Test Station
China Lake, California
ATTN: Technical Library

Commander
U. S. Naval Air Missile Test Center
Point Mugu, California

Headquarters
U. S. Air Force
Washington 25, D. C.

Department of the Air Force
Deputy Chief of Staff for Development
The Pentagon, Washington 25, D. C.
ATTN: Director of Research and Development

Commander
Air Research and Development Command
Andrews Air Force Base
Washington 25, D. C.

Commander
Air Materiel Command
Wright-Patterson Air Force Base, Ohio

Commander
Rome Air Development Center
Griffiss Air Force Base, New York

Air Force Cambridge Research Center
Bedford, Massachusetts
ATTN: R. Roberts

Commander
Armed Services Technical Information Agency
Arlington Hall Station
Arlington 12, Virginia
ATTN: TIPDR (10 copies)

Commandant
U. S. Marine Corps
Washington 25, D. C.

National Aeronautics and Space Administration
1520 H Street N. W.
Washington 25, D. C.
ATTN: Div of Research Information

National Security Agency
Fort George G. Meade, Maryland
ATTN: T. A. Prugh

National Bureau of Standards
Washington 25, D. C.
ATTN: Library

Boulder Laboratories
National Bureau of Standards
Boulder, Colorado
ATTN: Library

U. S. Atomic Energy Commission
Washington 25, D. C.
ATTN: Technical Reports Library

Director
Advanced Research Projects Agency
Washington 25, D. C.
ATTN: Chief, Technical Operations Div

Sandia Corporation
Sandia Base
Albuquerque, New Mexico

Los Alamos Scientific Laboratory
Los Alamos, New Mexico
ATTN: R. Watt/J-16

U. S. Atomic Energy Commission
Germantown, Maryland
ATTN: Div of Military Applications (DMA)

Horton, B. M. /McEvoy, R. W. , Lt Col,
   Apstein, M. /Gerwin, H. L. /Guarino, P. A. /Kalmus, H. P. /Schwenk, C.C.
Hardin, C. D. , 100
Sommer, H. , 200
Hatcher, R. D. , 300
Hoff, R. , 400
Nilson, H. , 500
Flyer, I. N. ,600
Campagna, J. H., 700
DeMasi, R. , 800
Landis, P. E. , 900
Seaton, J. W. , 260
Scales, J. , 920
Barnett, C. W. H. , 920
Allen, F. , 940
Klute, C. H. , 920
Kaiser, Q. C. , 920
Hall, L. L. , 920
Harrison, E. H. , 920
Svanholm, J. K. V., 920
Williams, D. , 920
Doctor, N. J. , 920
Horsey, E. F. /Benderly, A. A. , 910
Lucey, G. K. (30 copies)
Technical Reports Unit, 800
Technical Information Office, 010 (10 copies)
HDL Library (5 copies)

(Two pages of abstract cards follow.)